HIGHLIGHTS

- The comparison of the spectra of adsorbed thymine with the corresponding spectra of thymine in solution at pH 1, 7 and 12 indicates that adsorption involves the deprotonation of thymine in the whole pH range.
- The assignments of the ATR-SEIRAS signals in the 1400-1800 cm^{-1} region in the light of DFT calculations indicate that the N3 tautomer is the predominant adsorbed species in the experiments in acid media while the adsorbed N1 tautomer predominates in the case of the adsorption from basic media, but both species can be distinguished in the adsorption at pH 7.
- The analysis as a function of the potential of the relative intensities of the signals in the 2800-3300 cm^{-1} region at pH 1 permits to conclude that the N3 tautomer interacts with the surface by the C2O group at low chemisorption potentials and it rotates to interact also by the N3 atom and the C4O group as the potential is increased.
- The analysis as a function of the potential of the relative intensities of the signals in the 2800-3300 cm^{-1} region at pH 12 allows us to conclude that the N1 tautomer interacts with the metal in all the chemisorption region by the N1 atom and the C4O group.

Graphical Abstract (for review)

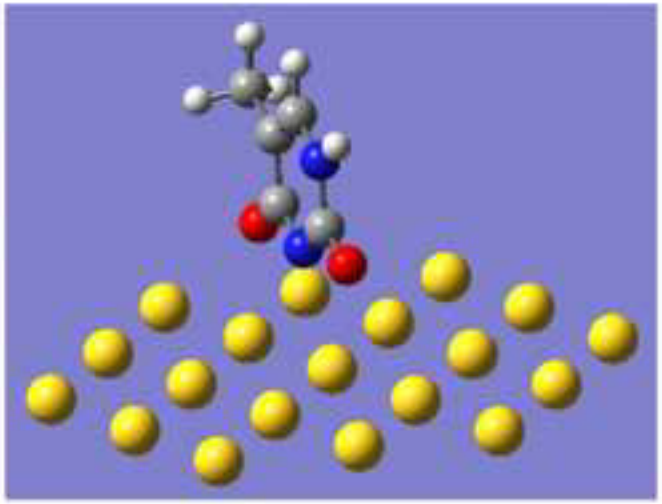

pH 1

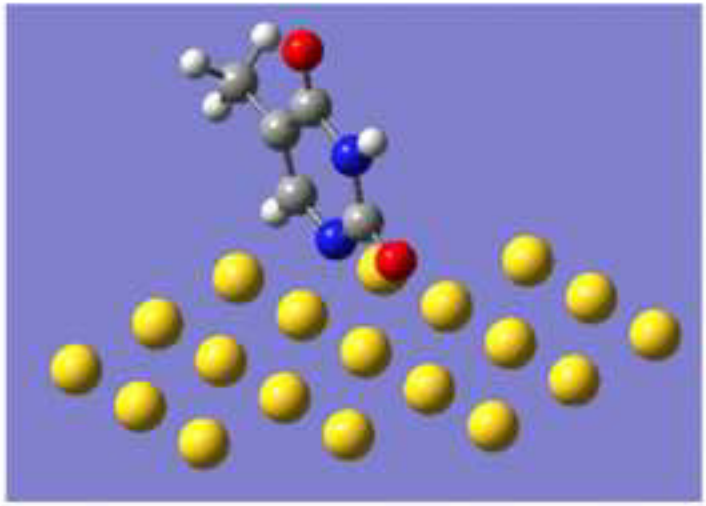

pH 12

TAUTOMERISM OF ADSORBED THYMINE ON GOLD ELECTRODES: AN IN SITU SURFACE-ENHANCED INFRARED SPECTROSCOPY STUDY.

F. Prieto*[(a)] , J. Alvarez-Malmagro[(a)], M. Rueda[(a)], J.M. Orts[(b)]

[(a)]*Department of Physical Chemistry. University of Seville*. *C/ Profesor García González nº 2, 41012 Seville (Spain).* phone: +34 954557174, e-mail: dapena@us.es

[(b)] *Department of Physical Chemistry and University Institute of Electrochemistry. University of Alicante. Ap. 99, E-03080, Alicante (Spain)*

ABSTRACT

The adsorption of thymine on gold electrodes has been studied by ATR-SEIRAS in situ spectroscopy at three pH values (1, 7 and 12), in order to analyse the tautomeric equilibrium of deprotonated thymine in the adsorbed state. The anionic form which is deprotonated in nitrogen N1 (N1 tautomer) and the one deprotonated in nitrogen N3 (N3 tautomer) are considered. The spectroscopic results have been interpreted in the light of DFT ab-initio calculations of both tautomeric forms adsorbed on gold surfaces. The basis sets 6-311++G(d,p) for C, H, O and N atoms and LANDL2DZ for Au atoms have been used. The electrode surface has been simulated as an unreconstructed Au(111) surface of 19 atoms.

The preponderance of each tautomer of adsorbed thymine as a function of pH has been inferred from the analysis of the spectral signals in the 1500-1800 cm^{-1} wavenumber region related mostly to stretching modes of the carbonyl groups. It has been found that the adsorbed N3 tautomer predominates in the case of adsorption from acid media while the N1 tautomer predominates in the adsorption from basic media but the adsorption of both forms have been distinguished in the experiments from neutral media. Moreover, the plausible changes in the orientation of the two

adsorbed tautomers with the electric field have been determined by analysing the relative intensities of the characteristic CH stretching signals in the 2800-3300 cm^{-1} spectral region. It is proposed that the N3 tautomer undergoes changes in the interaction sites with the metal and in the molecular plane orientation on the electrode as the electric potential is increased, but the N1 tautomer molecule keeps the interaction sites while the molecular plane slightly rotates to facilitate the electrostatic interaction with the field.

1.- INTRODUCTION

The biological relevance of DNA bases and the similarities between electrode/electrolyte interfaces and biological interfaces make the study of adsorption of DNA bases on electrodes an interesting task in order to understand the behavior of these molecules in the presence of static electric fields. The interactions between complementary basis by hydrogen bonds [1,2] play an important role in the right replication of the genetic material. The specificity of these intermolecular interactions can be affected by the tautomerism of the DNA bases involved: the existence of "unstable" tautomeric forms is considered one of the factors inducing the interactions between non complementary bases and, therefore, genetic mutations [3-8]. Several environmental or structural parameters can affect the stability of different tautomers of DNA bases, like the substitution with bromine or methyl group, the pH or the static electric field. Moreover, the acid-base properties of DNA bases can be affected by the presence of electric fields[9-12].

Thymine is involved in an acid-base equilibrium in aqueous solutions with a pKa value of 9.6. Deprotonation of thymine can take place either on the N1 or N3 atom, yielding two anionic species that are related by a tautomeric equilibrium, as it is shown in Scheme 1.

- Scheme 1 –

Wierzchowski studied this tautomeric equilibrium of deprotonated thymine by UV-vis and FT-IR spectroscopies, concluding that both tautomers are present in a similar concentration in basic aqueous solutions and that the N1 tautomers is favored decreasing the dielectric constant of the solvent [13].

On the basis of DFT calculations and including solvation effects Giese found that for deprotonated uracil, the higher charge dispersion in the tautomer N1 makes it more stable in gas phase, while the higher dipole moment of the tautomer N3 increases its relative stability in the presence of polar solvents, and probably under static electric field [14]. In aqueous media both tautomers exhibit close theoretical stabilities, although N1 tautomer is slightly more stable. Goddard et al. [15] estimated by DFT calculations the pKa values of different 5-substituted uracil derivatives, including thymine, and found that N3 tautomers of the deprotonated uracil derivatives are slightly more stable than the N1 tautomers.

The adsorption of thymine on gold single crystal electrodes has been studied by Roelfs et al by classical electrochemical methods, ex-situ XPS, in-situ STM and in-situ Fourier Transform Infrared Reflection Absorption Spectroscopy (FT-IRRAS) in the external reflection configuration [16,17]. Three different adsorption states were found, depending on the electric potential applied to the electrode, from lower to higher potentials: (I) a random physically adsorbed state, (II) a condensed physically adsorbed layer of thymine molecules oriented with the molecular plane parallel to the electrode surface and (III) a chemically adsorbed condensed layer with the molecular plane oriented normal to the electrode surface. The relative stability of these adsorption states is also strongly dependent on the crystallographic orientation of the single crystal electrode surface [16]. Moreover, the potential at which the transition between states (II) and (III) takes place varies nearly linearly with the pH value of the electrolyte, so it has been proposed that this transition involves the deprotonation of neutral thymine [16]. From the analysis of the two FT-IRRAS bands found in the region of 1450-1800 cm^{-1}, and from the XPS results, the authors proposed that the

deprotonation takes place on the nitrogen N3 and it is accomplished by a change in the orientation of the molecular plane, from parallel to normal to the electrode surface, in order to interact to the electrode by the two carbonyl groups and the nitrogen N3 [17].

ATR-SEIRA spectroelectrochemical measurements provide a high signal to noise ratio as compared to external reflection measurements, mainly because of the surface enhancement of the absorption and because of the lower influence on the spectra of the species in solution. [18]. In a previous work [19] we applied in-situ surface enhanced infrared reflection absorption spectroscopy, in the attenuated total reflection configuration (ATR-SEIRAS) to the co-adsorption of thymine and adenine, concluding that both complementary bases change their orientation relative to the electrode in the presence of the other base, as compared when they are adsorbed separately: adenine adopts a more upright position and thymine becomes parallel to the electrode surface. These changes have been explained as a consequence of the intermolecular interactions between complementary DNA bases.

Cho et al. [20] combined surface enhanced Raman scattering spectroscopy and DFT calculations to the study of adsorption of thymine on gold and silver nanoparticles, concluding that in the adsorbed state the more stable tautomer is N3, although they also detected the N1 tautomer adsorbed on silver nanoparticles.

The high resolution and sensitivity of ATR-SEIRAS “in situ” measurements, using a Kretchsmann design of the electrochemical cell, have been used to determine different aspects related to the pH dependence of adenine adsorption on gold electrodes [12,21]: the presence of physisorbed protonated adenine has been detected at very low pH values and electrode potentials [21]. Moreover, the deconvolution of the

signals due to chemisorbed adenine in the neutral – basic pH range has allowed the evaluation of the second pKa of adenine at the electrode/electrolyte interface [12].

In this article, the adsorption of thymine on gold electrodes is studied by ATR-SEIRA in situ spectroscopy in a wide pH range in order to analyze the tautomeric equilibrium of the adsorbed thymine , which can help to better understand the interactions with the different adsorbed forms of adenine. The spectroscopic results have been interpreted in the light of DFT calculations of both tautomeric forms adsorbed on gold surfaces. The higher sensitivity of the spectroelectrochemical technique has allowed us to analyze the preponderance of each tautomer of thymine as a function of pH. Moreover, the influence of the electric field on the molecular plane orientation and the interaction sites with the metal of the two adsorbed tautomers have been determined by analysing the characteristic CH stretching signals in the 2800-3300 cm^{-1} spectral region and the results have been explained on the basis of the electrostatic interaction energy with the permanent dipole moment.

2.- EXPERIMENTAL

2.1.- Reagents and electrodes

Solutions were prepared either in ultra pure water from a Millipore Direct-Q purifier or in deuterium oxide (Sigma 99.99 %). The supporting electrolytes used were 0.1 M $HClO_4$, $KClO_4$ or $KClO_4$ + NaOH. Sodium hydroxide, perchloric acid and potassium perchlorate were from Merck Suprapur®. Thymine, from Sigma, was used without further purification. Stock solutions of thymine 10 mM were prepared in the same

supporting electrolyte and spikes were added to the cell solution in order to get the desired working thymine concentration. All the solutions were deareated by bubbling argon (Air Liquide N50) during 30 min. prior to use.

Voltammetric experiments were performed with an Autolab PGstat 30 multipurpose electrochemical system, controlled by NOVA 1.7 software. The working electrode was a freshly flame annealed Au(111) single crystal electrode prepared following the procedure described by Clavillier [22]. A gold wire and a saturated mercury/mercurous sulphate electrode connected to the cell via a salt bridge were used as auxiliary and reference electrodes respectively. Solution's pH was measured with a PHM 64 pH meter from Radiometer and a Hamilton borosilicate membrane combined electrode. The pH readings on deuterium oxide solutions were corrected according to [23]. All the potentials are given vs. SCE.

2.2.- Spectroelectrochemical measurements

FT-IRRAS spectra were obtained at a resolution of 4 cm^{-1} with a NICOLET 6700 spectrophotometer equipped with a narrow-band MCT-A detector cooled with liquid nitrogen, and a V-max II accessory for reflectance measurements. The spectra were collected either with p or s polarized radiation, selected with a ZnSe motorized polarizer, and are presented as the ratio $-\log(R/R_0)$ with R and R_0 being the reflectance spectra at the sample and reference conditions, respectively. Electrochemical control of the cell was made with a CHI 1100 A potentiostat from CH Instruments.

ATR-SEIRA spectra were obtained using the Kretchsmann configuration of the spectroelectrochemical cell: the cell window consisted in a silicon prism beveled at 60^0.

The working electrode was a gold film deposited on to a face of the silicon prism by argon sputtering with a Leica EM SCD500 metalizer equipped with a quartz crystal microbalance to control the thickness and the speed of deposition (c.a. 25 nm and 0.01 nm s^{-1}). The three electrode cell was completed with the same reference electrode as in the voltammetric measurements and a gold foil acting as auxiliary electrode. The spectra measured can be referenced either to a potential at which thymine is desorbed or at the same potential but in the absence of thymine in the bulk solution. Every spectrum was obtained averaging 100 interferograms.

ATR infrared absorption spectra of thymine in solution were measured with a cell equipped with a ZnSe prismatic window beveled at 45º. Each spectrum is obtained averaging 1000 interferograms, and is referred to the single beam spectrum obtained for the corresponding solvent (either H_2O or D_2O) under the same conditions.

2.3.- Computational details.

The geometry and vibrational properties of adsorbed thymine on gold electrode surfaces have been modeled using an unreconstructed Au(111) surface of 19 atoms. The size is big enough as to avoid the bonding of the adsorbate to edge atoms during the geometry optimization. The geometry of the gold surface or cluster was kept fixed. Geometry optimization of adsorbed thymine and the theoretical estimation of its harmonic vibrational frequencies were performed with a PBE functional as implemented in the Gaussian 09 software and the basis sets 6-311++G(d,p) for C, H, O and N atoms and LANDL2DZ for Au atoms. Unix version of Gaussian 09 running on a Fujitsu Primergy cluster was used.

3.- RESULTS AND DISCUSSION

3.1. –Cyclic voltammetry.

In figure 1 are shown the cyclic voltammograms obtained for 1mM thymine solutions at three different pH values. The different adsorbed states described by Roelfs et al. [16] are clearly distinguished at pH 1, with the pairs of transition peaks T1 and T1*between adsorption states (I) and (II) and of peaks T2 and T2*corresponding to the transition between the adsorption states (II) and (III). The potentials of T2 and T2* transition peak shift as the pH increases in the way of making shorter the potential range of the adsorption state (II), until it finally disappears at high pH values.

- Fig. 1-

3.2.- FT-IR spectra of thymine in solution.

In figure 2 are shown the transmission spectra of 10 mM thymine solutions at three different pH values in the 1500-1800 cm^{-1} spectral range, either in D_2O or in H_2O. This spectral region includes, in the case of deuterated media, the high intensity bands corresponding to the two CO and the C_5-C_6 stretching vibrations and some low intensity bands assigned to CH or CH_3 bending modes. The spectrum obtained in D_2O solutions at pH 12 has the same features as the spectrum obtained by Wierzhowski for thymine in 0.01 M NaOD in D_2O [13]. In the case of non-deuterated aqueous media this spectral region includes also NH and OH bending modes (the later one from the solvent). The spectral region around 2800-3200 cm^{-1} provides the CH and NH stretching modes but their transition dipoles are low so they are very weak bands.

Although the absorption bands corresponding to N-H (or N-D) stretching vibrations are of great interest, their low intensities and the interference with the O-H (or O-D) stretching bands from the solvent do not allow us to clearly detect these bands in the spectra of thymine in non-deuterated aqueous solutions.

It can be observed in Fig. 2 that the spectra at neutral and acid pH values are essentially the same but at pH 12 the spectral characteristics in the 1500-1800 cm^{-1} are rather different. These observations are in agreement with the acid-base equilibrium of thymine represented in scheme 1, with a pKa value of 9.6, so the spectra at pH (or pD) 1 and 7 correspond to the neutral form of thymine, while the spectrum at pH 12 is related the deprotonated anionic thymine species.

The assignments of the main characteristic bands of the spectra based on our DFT calculations are given in Table I in comparison with the experimental spectra obtained in D_2O media and in H_2O media. The theoretical frequencies for neutral thymine are comparable to the values and assignment reported by Chandra [24] calculated with a B3LYP /6-31 ++G(d,p) theory level, taking into account the differences in the corresponding scaling factors [25], and to the experimental spectrum of thymine in Ar an N_2 matrix [26][1].The experimental frequencies obtained in acid and neutral media are close to the calculated for neutral thymine. In non-deuterated thymine the calculated signals at this spectral region include contributions form NH bending modes, that in deuterated thymine (formed by exchange with the D_2O solvent) are shifted to lower wavenumbers. The slightly lower frequency values of the experimental signals of the C2O, C4O and C5C6 stretching modes can be ascribed to hydrogen bonding interactions of thymine in solution. In fact, the inclusion of two water molecules in the

computational chemistry calculations makes the theoretical frequencies closer to the experimental ones. Giese et al. found a similar influence of the hydration of uracil on the DFT calculated Raman frequencies [14], and by Chandra for the interaction of thymine with one water molecule [24][2] with B3LYP/6-31^{++} G(d,p) theory level

- Table I-

The frequencies of the spectral bands obtained in deuterated aqueous media at pH 12 are in good agreement with the calculated modes for either the N1 or the N3 deprotonated thymine tautomers. In non deuterated conditions at pH 12 the experimental wide band obtained at 1600 cm^{-1} could be a combination of signals of both tautomeric forms overlapped by the intense uncompensated OH bending band due to the solvent at this high pH.

These results suggest that in basic solutions both tautomeric forms of deprotonated thymine are present, in good agreement with the conclusion of Wierzchowski [13].

The CH and CH_3 stretching modes in the 2850-3200 cm^{-1} spectral region do not show any apparent influence from the protonation degree or from the isotopic substitution. Three active absorption bands are obtained at c.a. 2955 cm^{-1}, 2927 cm^{-1} and 2851 cm^{-1}. The calculated vibrational frequencies for neutral and for anionic thymine molecules are higher than the experimental ones but the differences can be eliminated with the scaling factor reported for CH stretching vibrations calculated with the functional and basis sets used [25].

3.3.- ATR-SEIRAS of thymine adsorbed on gold electrodes.

3.3.1.- Region of carbonyl groups stretching vibrations at high potentials.

In figure 3 are shown the 1450-1800 cm^{-1} ATR-SEIRA spectra of thymine adsorbed on gold nanofilm electrodes at potentials higher than the onset of the chemisorption of thymine at three limiting pH values in D_2O (figure 3a) and in H_2O (Figure 3b). For the sake of comparison, the spectra obtained in solution at the same experimental conditions have been included. It can be observed that the bands show higher signal to noise ratios than in the spectra of thymine in solution and higher sensitivity than in the SNIFTIR spectra obtained for adsorbed thymine on Au(111) electrodes from high thymine bulk concentration solution [17]. The surface selection rules require that any ATR-SEIRAS active vibration has a transition dipole moment with a component normal to the electrode. Therefore, as all the vibrations in the range 1450-1800 cm^{-1} correspond to in-plane modes, the molecular plane of adsorbed thymine cannot be oriented parallel to the electrode surface but it should be at least tilted on the surface

The ATR-SEIRA spectra in the region 1450-1800 cm^{-1} exhibit a clear pH dependence in the two solvents: in D_2O and acid media a medium intensity absorption band appear at 1648 cm^{-1} , a strong band at 1581 cm^{-1} (shoulder at 1567 cm^{-1}) and a weaker one at 1478 cm^{-1} while in basic media three overlapped signals can be distinguished at 1627 cm^{-1} , 1573 cm^{-1} and 1521 cm^{-1} (the band of higher frequency being also the stronger one), and a weak signal at 1413 cm^{-1}. In H_2O the ATR-SEIRAS spectrum in acid media shows two strong signals at 1656 cm^{-1} and 1597 cm^{-1} and a weak one at 1490 cm^{-1}, while in basic media a strong and wide band, centered at 1643 cm^{-1} is the most characteristic feature in the spectrum. At first sight, the differences in the spectra obtained at pH 1 and 12 can indicate that the adsorbed species responsible for the absorption signals are different at each pH value or alternatively, that the same species is responsible for the absorption at both pH values but with different orientations of

the molecular plane relative to the reflection surface. Curiously, at pH 7 the ATR-SEIRA spectra obtained either in D_2O or in H_2O include signals which are present in the spectra at the respective two limiting pH values (1 and 12), so the spectra at pH 7 can be expressed as linear combination of the spectra at pH 1 and 12 (figure 3a). These observations suggest the existence of two different adsorbed species at pH 1 and 12 that are both co-adsorbed on the electrode at pH 7. Two possibilities can be envisaged about the nature of the two pH-dependent adsorbed species: either the neutral and one of the deprotonated thymine forms (acid-base equilibrium) or the deprotonated species in N1 and N3 (tautomeric equilibrium). The presence of an adsorbed neutral thymine form was already discarded by Roelfs et al. even in very acid media on the basis of electrochemical STM, in-situ SNIFTIRS and ex situ XPS measurements of thymine adsorbed on gold electrodes [16,17]. They proposed a model for chemisorption of thymine from acid media with the N3 deprotonated molecule oriented upright on the electrode surface with N3 and both carbonyl groups interacting with the electrode. Then, the pH dependence found for the potential onset of thymine chemisorption on gold in the pH range 1 to 12 observed in Figure 1 cannot be related to an acid-base equilibrium. Moreover, the comparison in Figure 3 of the spectra of adsorbed thymine with those of thymine in solution shows clear differences in the behaviors at pH 1 and pH 12. The signals in the ATR-SEIRAS spectrum at pH 12 are blue-shifted with respect to the signals in the spectrum of thymine in solution and this change can be explained as a consequence of the interactions of the carbonyl groups with the metal in the case of the adsorbed species, so it is feasible that at pH 12 the same forms of thymine that are present in solution get adsorbed on the electrode. On the contrary, the ATR-SEIRAS signals of adsorbed thymine from pH 1 solutions are

red-shifted with respect to the signals in the spectrum of thymine in solution suggesting that different chemical species are responsible for the spectra: the neutral thymine form that is present in solution in acid media is responsible for the transmission and one of the deprotonated thymine form, more probably the tautomer in N3, as proposed by Roelfs et al. [16,17] for the ATR-SEIRA spectra. Therefore, apparently the nature of the deprotonated thymine tautomer which gets adsorbed on gold electrodes depends on the pH of the solution: if it is accepted that the N3 deprotonated tautomer get adsorbed from acid solutions, most probably the N1 deprotonated tautomer is the adsorbed species from basic solutions.

- Fig. 3a and 3b-

To confirm this hypothesis DFT calculations of N3 and N1 tautomers of deprotonated thymine on a cluster of 19 gold atoms have been performed. The optimized geometries are represented in scheme 2. Optimized N3 tautomer is oriented normal to the electrode surface, with both carbonyl groups and nitrogen N_3 directed towards the electrode. The molecular plane is slightly rotated (c.a. 10 degrees) relative to the closest main direction of the gold crystal. The distances between the nitrogen N_3 and the two oxygen atoms (O_7 and O_8) and the corresponding closest gold atom are 2.59 Å, 3.19 Å and 2.45 Å respectively, so the interaction with the electrode takes place mainly by N_3 and O_8. N1 tautomer is also oriented normal to the electrode in this case with N_1 and O_7 closer to the surface (2.77 Å and 2.89 Å to the closest gold atom in each case respectively).

- Scheme 2-

The vibrational frequencies in the region around 1600 cm^{-1} calculated for the optimized geometries of the adsorbed N3 and N1 deprotonated thymine tautomers are given in Table II in comparison to the experimental values obtained at pHs 1 and 12 in D_2O and in H_2O media. As was mentioned above this spectral region includes the CO and C=C stretching modes and the CH and NH bending modes. In the case of deuterated media the frequencies of the ND bending modes are shifted to lower wavenumbers beyond this spectral region.

-Table II-

The theoretical spectrum for the adsorbed deuterated N3 tautomer exhibits two strong absorption bands at 1640 cm^{-1} due mainly to the C5C6 stretching mode and at 1586 cm^{-1} due to the two carbonyl groups stretching modes and a weak signal at 1463 cm^{-1} originated by bending modes of methyl group and of CH bond which can be correlated with the bands of the experimental ATR spectrum obtained at pD=1 (two strong bands at 1648 cm^{-1} and 1581 cm^{-1} and a weak band at 1478 cm^{-1}). They are shifted to lower frequency values than in the calculated spectrum of the same tautomer in solution, indicating that the molecule interact with the metal by the atoms involved in these vibration modes. The calculations provide also a strong signal at 1414 cm^{-1} due mainly to C4O and C2O stretching modes that can be associated to the experimental band at 1440 cm^{-1}, although the experimental band is weak (any of the experimental spectra provide strong signals around this frequency). A similar correlation can be observed for the theoretical bands of the adsorbed N3 tautomer and the experimental ATR-SEIRA spectrum at pH 1 in H_2O: the calculated spectrum shows two strong bands at 1645 cm^{-1} (C5C6 stretching mode) and at 1599 cm^{-1}

(carbonyl groups stretching modes with some contribution of the N1H bending vibration in this case) and medium-weak bands at 1463 cm^{-1}, 1447 cm^{-1} and 1410 cm^{-1} that could correspond to the experimental ATR spectral signals obtained at 1656 cm^{-1}, 1597 cm^{-1},1490 cm^{-1}, 1440 cm^{-1} and 1403 cm^{-1}, respectively.

Regarding the theoretical spectrum of the adsorbed N1 deprotonated tautomer the deuterated form exhibits a very strong absorption band at 1624 cm^{-1} due to the C4O stretching mode and two weak bands at 1558 cm^{-1} and 1483 cm^{-1} due mainly to the C2O and the C5C6 stretching modes, respectively which can match well the experimental spectra at pD=12 that show a strong and wide band at 1627 cm^{-1} and weak bands at 1573 and 1521 cm^{-1}. In non-deuterated aqueous media the experimental spectrum at pH 12 contains an strong and wide band at 1643 cm^{-1}, that correlates properly with the calculated frequency of 1639 cm^{-1} of the N1 tautomer (due to a mode that contains contributions of the C4O stretching vibration and of the N3H bending vibration), two very weak bands at 1558 cm^{-1} and 1506 cm^{-1}, than can be identified with the calculated frequencies at 1567 cm^{-1} (due to a mode with contributions of C2O stretching and N3H bending vibrations) and 1493 cm^{-1} (with contributions of C5C6 and C2C3 stretching and CH3 bending vibrations), respectively.

The assignation of the calculated vibrational frequencies to the different normal modes is included in Table II. It must be noted here that most of the calculated frequencies in the 1400-1800 spectral region result from the combination of contributions of different single vibration modes.

3.3.2.- Spectral Region of methyl and methenyl stretching vibrations at high potentials.

At wavenumbers between 2850-3100 cm^{-1} the weak bands corresponding to stretching modes of CH_3 and are shown in figure 4 in deuterated media. In H_2O media the proximity of the OH stretching bands of the solvent diminishes the signal to noise ratio. The comparison with the absorption spectra in solution, either at pD 1 or pD 12, reveals that the bands due to the adsorbed species are shifted towards higher wavenumbers, as expected for stretching vibration modes. The experimental spectra obtained at the two limiting pD values (1 and 12) can be deconvoluted into three Lorentzian bands, that show changes in the relative height of the bands with the pD value. Moreover a change in the frequencies of the two bands at lower wavenumbers is also found from pD 1 to 12. At intermediate pD values the experimental spectrum is a combination of the spectra obtained at the two limiting pD values. Assuming for adsorbed thymine a molecular plane orientation perpendicular to the electrode surface these bands must correspond to two stretching vibrations of the methyl group (the symmetric vibration and the in-plane anti-symmetric vibration with an in-plane component of the transition dipole) and to the methenyl stretching vibration. The remaining anti-symmetric methyl stretching out of plane vibration would have a transition dipole which is normal to the molecular plane so it is not an active vibration mode in the IRRAS configuration for the assumed molecular orientation.

- Fig. 4-

In Table II the calculated frequencies for the adsorbed N3 and N1 deprotonated thymine tautomers are compared to the experimental frequencies obtained at pD 1 and pD 12 by deconvolution of the spectrums exhibited in figure 4. The differences in the calculated frequency values for the two tautomers are within the scaling factor

uncertainties reported for ab initio vibrational frequencies [25], so they cannot be used to ratify the nature of the tautomeric form that get adsorbed from each pD medium. However, the calculations allow the assignment of the experimental bands. In this respect, it is to be noted the significant differences in the calculated wavenumbers of the CH and anti-symmetric CH_3 stretching vibrations obtained for each tautomers (see Table II): the highest wavenumber for the N3 tautomer spectrum corresponds to the CH stretching mode while for the N1 tautomer it is due to the anti-symmetric CH_3 in plane stretching mode. This effect is also found in the ab initio calculated vibrational frequencies of the two tautomers in solution. Therefore, the experimental bands of the spectra at pD 1 and at pD 12 have been assigned according to the calculations for the N3 and the N1 tautomers, respectively. The assignments have been illustrated in Figure 4.

3.4.- Influence of potential in the orientation of adsorbed thymine on gold electrodes.

The ATR-SEIRA spectra of adsorbed thymine on gold electrodes from deuterated solutions at pD 1 and pD 12 at some indicated potentials are represented in figures 5a and 5b respectively. At pD 1 and at potentials lower than the onset of thymine chemisorption (peak T2 in figure 1) the characteristic bands of adsorbed thymine in the regions around 1600 cm^{-1} and around 3000 cm^{-1} do not show up in the spectra, indicating that physisorbed thymine is oriented with the molecular plane parallel to the electrode surface. As the potential becomes closer to the chemisorption region (but still in the condensed phase II potential region) these bands appear and their

height increase with the potential. At potentials higher than 0.3 V the overlapped bands around 1570- 1580 cm^{-1} clearly develop with relative heights that are potential dependent: the development with potential of the band at 1585 cm^{-1} is higher than that of the other two bands in that region. A similar behavior can be observed in the spectral signals around 3000 cm^{-1}, but in this case the heights of the two signals of higher wavenumbers increase more with potential than that of the one at 2960 cm^{-1}. At sufficiently high potential values the spectra become independent on the applied potential.

- figures 5a and 5b -

A different behavior with potential is found in the ATR-SEIRA spectra of adsorbed thymine on gold from pD 12 solutions. Although the corresponding in-plane vibration signals for adsorbed thymine increase with the potential, they show up at very low potentials far from the onset of thymine chemisorption, indicating that contrary to the case of physisorbed thymine at pD 1, in basic media the molecule is not oriented parallel to the electrode but it has some inclination. Moreover, in this media the changes in the relative heights of the signals with the potential are less significant: all of the signals seem to grow up at the same ratio as the potential is increased.

The changes in the relative intensities of the bands of the spectrum of each adsorbed thymine tautomer with potential can be used to determine the plausible changes in their molecular orientations on the electrode induced by the electric field. The integral intensity of a reflection-absorption band of a film of adsorbed molecules, obtained with linearly polarized light at the normal direction of the reflection surface, Ap, is

proportional to the scalar product of the transition dipole vector and the electric field of the photon, so it can be expressed as [27]:

$$A_p \quad \propto \quad \Gamma \left| \vec{\mu} \times \vec{E}_p \right| = \Gamma \left| \mu \right|^2 \left\langle E_p^2 \right\rangle \cos^2(\theta) \qquad (1)$$

Where Γ is the surface concentration of the molecule responsible for the light absorption, θ is the angle between the transition dipole and electric field of photon vectors that for p-polarized radiation have a direction normal to the electrode surface, $|\mu|$ is the transition dipole modulus and $\langle Ep^2 \rangle$ is the mean square intensity of the electric field of p radiation at the reflection surface. The change in the intensities of the spectral bands with the potential can be caused by an increase in the surface concentration and a change in the molecular orientation and therefore in the angle between the corresponding transition dipole moment and the normal direction to the electrode. The other two parameters in equation two, $\langle Ep^2 \rangle$ and $\langle \mu \rangle$, are independent of the potential. Then, the ratio between the integral intensities of two reflection absorption bands is proportional to the ratio of the squared cosines of the angles between each of the transition dipoles and the normal direction to the electrode:

$$\frac{A_p^{\bar{\nu}_1}}{A_p^{\bar{\nu}_2}} \quad \propto \frac{\cos^2(\theta^{\bar{\nu}_1})}{\cos^2(\theta^{\bar{\nu}_1})} \qquad (2)$$

Therefore, if the directions of the associated transition dipoles of two independent bands are known from DFT calculations it is possible to infer the changes of the molecule orientation with the potential, from the potential dependence of the ratio between the corresponding integral intensities.

The bands at c.a. 1500-1700 cm^{-1} (of CO and CC stretching modes) have higher signal to noise ratios than the bands at c.a. 2900-3100 cm^{-1} (of the CH stretching modes). However, the calculated vibrations for the signals around 2900-3100 cm^{-1} involve the assignment of individual modes with clear directions for their transition dipoles, while the signals around 1500-1700 cm^{-1} have contributions from different stretching modes and the uncertainty into the relative contribution of each individual mode originates a great ambiguity in the corresponding transition dipole directions. Therefore, the influence of the electrode potential on the molecular orientation of each adsorbed thymine tautomer has been analyzed using the integrated intensities of the bands corresponding to the methyl and the methenyl stretching modes.

- Fig 6a and Fig 6b-

In figure 6a the integrated intensities of the ATR-SEIRAS bands obtained at pD 1 at 3070 cm^{-1} and at 2985 cm^{-1} which have respectively been assigned to the C6H stretching and anti-symmetric CH_3 stretching modes of the N3 deprotonated thymine tautomer, in relation to the integrated intensity of the symmetric CH_3 stretching band (at 2960 cm^{-1}) are plotted as a function of potential. In both cases, as the potential increases the ratio of integrated intensities increases reaching a maximum value at high potentials. Both vibrations, at 3070 cm^{-1} and 2985 cm^{-1}, have transition dipole moments with directions close to the virtual axis between N3 and C6 while the vibration at 2960 cm^{-1} has a moment direction close to the virtual axis between C2 and C5 (see scheme 3a). Then a similar behavior with potential must be expected for both integrated intensities related to the 2960 cm^{-1} band, as experimentally observed. The changes of the relative intensities shown in figure 6a suggest that as the potential

increases the adsorbed N3 deprotonated thymine molecule rotates so the axis N3-C5 gradually becomes more normal to the electrode surface as compared to the axis C2-C5. Therefore it can be proposed that at lower potentials in the chemisorption region the molecule interacts with the electrode by the oxygen atom of carbonyl C2O group and as the potential increases the rotation of the molecular plane facilitates the additional interactions by the N3 atom and the oxygen of the C4O group. The driving forces for this rotation include both the chemical interaction with the gold surface by N3 and C4O and the electrostatic interaction between the increasing permanent electric field and the permanent dipole of the N3 deprotonated thymine tautomer, directed from N3 to C6.

- Scheme 3 -

The ATR-SEIRAS of thymine adsorbed on gold electrodes from pD 12 solutions show a lower signal to noise ratio in the region of methyl and methenyl stretching bands and the potential window used must be shortened in order to avoid the oxidation of the gold film. However, it is still possible to perform with the data at pD 12 a similar analysis of the potential influence on the orientation of thymine molecule adsorbed as it has been shown above for the data at pD 1. The integrated intensities of the ATR-SEIRAS bands obtained at pD 12 at 2977 cm^{-1} and at 3072 cm^{-1} that correspond to the C6H and anti-symmetric CH_3 stretching modes of N1 deprotonated thymine, in relation to the integrated intensity of the symmetric CH_3 stretching band (at 2926 cm^{-1}) are plotted against the potential in figure 6b. At potentials higher than the onset of the chemisorption, c.a. 0 V vs SCE, both ratios show a weak decrease as the potential increase, indicating a short degree of rotation of the molecular plane so the axis from

C6 to N3 becomes gradually less normal to the electrode as compared to the axis from C2 to C5, as is represented in scheme 3b. This can be explained assuming that the chemisorption of the N1 deprotonated thymine tautomer implies the interaction of the nitrogen N1 and the oxygen of the C2O group with the electrode, as predicted by the DFT calculations, so the molecule plane is oriented accordingly. In this orientation the permanent dipole of the molecule, which is directed from C2 to C5, is almost aligned with the electric field at the interface so only slight rotations of the molecular plane are needed when the electrode potential is increased in order to facilitate the electrostatic interactions of the permanent dipole of the molecule with the electric field, the interaction sites of the molecule with the metal remaining the same in all the chemisorption potential range.

4.- CONCLUSIONS

ATR-SEIRAS in situ spectroelectrochemical experiments of adsorbed thymine at pH 1, 7 and 12 in D_2O and H_2O media have allowed us to analyse the tautomerism of the adsorbed thymine anionic forms as a function of pH. The comparison of the spectra recorded at high potentials in the chemisorption regions with the respective spectra of thymine in solution at the three pH values indicates that the species adsorbed from acid and neutral media are others than the neutral thymine form existing in solution at pH bellow the pKa value. Deprotonation of thymine coupled to the adsorption process is then concluded based also on experimental electrochemical evidences even at pH values very much bellow the pKa value. The resulting anionic thymine forms can be the N1 and/or the N3 tautomers. The assignment of the signals in the 1400-1800 cm^{-1}

spectral region in the light of DFT calculations for the individual deuterated and non-deuterated molecules and for the same adsorbed molecules on gold surfaces indicate that the N3 tautomer is the predominant adsorbed species in the experiments in acid media while the adsorbed N1 tautomer predominates in the case of the adsorption from basic media, but both species can be distinguished in the adsorption at pH 7.

The influence of the electric field on the orientations and interaction sites of the adsorbed molecules with the metal have been inferred from the analysis of the relative intensities of the characteristic CH stretching signals in the 2800-3300 cm^{-1} spectral region. It is concluded that the N3 tautomer molecule probably rotates modifying the interaction sites from only the C2O group at low potentials in the chemisorption region to include also the N3 atom and the C4O group as the potential is increased to finally adopt the chemically more stable configuration and the most favourable alignment of the permanent dipole moment of the molecule with the electric field. However, the N1 tautomer molecule probably interacts with the metal in all the adsorption potential region by the N1 atom and the C4O group, in accordance with the most stable configuration provided by the calculations and also with the electrostatic interactions with the electric field, as the permanent dipole moment of the molecules is almost aligned with the electric field in this configuration. Only slight rotations of the molecular plane with the electric potential are proposed

ACKNOWLEDGEMENTS

Financial support from the Spanish Ministry of Economy and Competitiveness (CTQ2014-57515-C2-1-R and CTQ-2013-44083-P) and from the Junta de Andalucia (PAI FQM202) is gratefully acknowledged.

The authors want to thank Centro de Servicios de Informatica y Redes de Comunicaciones (CSIRC) of University of Granada for the computing time. and the general services (CITIUS) of Seville University for the use of the sputtering metalizer equipment. JAM acknowledges a FPU grant from the Spanish Ministry of Science and Technology.

REFERENCES

[1] J.D. Watson, F.H.C. Crick, Molecular Structure of Nucleic Acids – A Structure For Deoxyribose Nucleic Acid, Nature. 171 (1953) 737–738. doi:10.1038/171737a0.

[2] K. Hoogsteen, The Structure of Crystals Containing a Hydrogenbonded Complex of 1-Methylthymine And 9-Methyladenine, Acta Crystallogr. 12 (1959) 822–823. doi:10.1107/s0365110x59002389.

[3] V.H. Harris, C.L. Smith, W.J. Cummins, A.L. Hamilton, H. Adams, M. Dickman, et al., The effect of tautomeric constant on the specificity of nucleotide incorporation during DNA replication: Support for the rare tautomer hypothesis of substitution mutagenesis, J. Mol. Biol. 326 (2003) 1389–1401. doi:10.1016/s0022-2836(03)00051-2.

[4] M. Rueda, F.J. Luque, J.M. Lopez, M. Orozco, Amino-imino tautomerism in derivatives of cytosine: Effect on hydrogen-bonding and stacking properties, J. Phys. Chem. A. 105 (2001) 6575–6580. doi:10.1021/jp010838o.

[5] W. Wang, H.W. Hellinga, L.S. Beese, Structural evidence for the rare tautomer hypothesis of spontaneous mutagenesis, Proc. Natl. Acad. Sci. 108 (2011) 17644–17648. doi:10.1073/pnas.1114496108.

[6] J.P. Ceron-Carrasco, D. Jacquemin, E. Cauet, Cisplatin cytotoxicity: a theoretical study of induced mutations, Phys. Chem. Chem. Phys. 14 (2012) 12457–12464. doi:10.1039/c2cp40515f.

[7] J.A. Kereselidze, Z. V. Pachulia, T.S. Zarqua, Quantum-chemical description of the prototropic tautomerism of pyrimidine bases, Chem. Heterocycl. Compd. 45 (2009) 680–684. doi:10.1007/s10593-009-0331-6.

[8] M. Orozco, B. Hernández, F.J. Luque, Tautomerism of 1-Methyl Derivatives of Uracil, Thymine, and 5-Bromouracil. Is Tautomerism the Basis for the Mutagenicity of 5-Bromouridine?, J. Phys. Chem. B. 102 (1998) 5228–5233. doi:10.1021/jp981005+.

[9] K. Gehring, J.L. Leroy, M. Guéron, A tetrameric DNA structure with protonated cytosine.cytosine base pairs., Nature. 363 (1993) 561–5. doi:10.1038/363561a0.

[10] A.M. Pyle, Metal ions in the structure and function of RNA., J. Biol. Inorg. Chem. 7 (2002) 679–90. doi:10.1007/s00775-002-0387-6.

[11] G.W. Muth, A Single Adenosine with a Neutral pKa in the Ribosomal Peptidyl Transferase Center, Science (80-.). 289 (2000) 947–950. doi:10.1126/science.289.5481.947.

[12] J. Álvarez-Malmagro, F. Prieto, M. Rueda, A. Rodes, In situ Fourier transform infrared reflection absorption spectroscopy study of adenine adsorption on gold electrodes in basic media, Electrochim. Acta. (2014) 1–6. doi:10.1016/j.electacta.2014.03.074.

[13] K.L. Wierzchowski, E. Litoñska, D. Shugar, Infrared and ultraviolet studies on the tautomeric equilibria in aqueous medium between monoanionic species of uracil, thymine, 5-fluorouracil, and other 2,4-diketopyrimidines., J. Am. Chem.Soc. 87 (1965) 4621–4629. doi:10.1021/ja00948a039.

[14] B. Giese, D. McNaughton, Surface-Enhanced Raman Spectroscopic Study of Uracil. The Influence of the Surface Substrate, Surface Potential, and pH, J. Phys. Chem. B. 106 (2002) 1461–1470. doi:10.1021/jp011986h.

[15] Y.H. Jang, L.C. Sowers, C. Tahir, W.A. Goddard, First Principles Calculation of pK a Values for 5-Substituted Uracils, J. Phys. Chem. A. 105 (2001) 274–280. doi:10.1021/jp994432b.

[16] B. Roelfs, E. Bunge, C. Schröter, Adsorption of thymine on gold single-crystal electrodes, J. Phys. Chem. B. 101 (1997) 754–765. doi:10.1021/jp961814y.

[17] W. Haiss, B. Roelfs, S.N. Port, E. Bunge, H. Baumgartel, R.J. Nichols, In-situ infrared spectroscopic studies of thymine adsorption on a Au(111) electrode, J.Electroanal. Chem. 454 (1998) 107–113. doi:10.1016/s0022-0728(98)00243-5.

[18] M. Osawa, In-situ Surface-Enhanced Infrared Spectroscopy of the Electrode/Solution Interface, in: R.C. Alkire, D.M. Kolb, J. Lipkowski, P. Ross (Eds.), Adv. Electrochem. Sci. Eng., Wiley-VCH Verlag GmbH, 2006: pp. 269–314. doi:10.1002/9783527616817.ch8.

[19] M. Rueda, F. Prieto, J. Alvarez, A. Rodes, Adenine-thymine interactions on gold electrodes studied by in-situ electrochemical FT-IR-spectroscopy, Febs J. 279 (2012) 515–516.

[20] K.-H. Cho, J. Choo, S.-W. Joo, Tautomerism of thymine on gold and silver nanoparticle surfaces: surface-enhanced Raman scattering and density functional theory calculation study, J. Mol. Struct. 738 (2005) 9–14. doi:10.1016/j.molstruc.2004.11.001.

[21] M. Rueda, F. Prieto, A. Rodes, J.M. Delgado, In situ infrared study of adenine adsorption on gold electrodes in acid media, Electrochim. Acta. 82 (2012) 534– 542. doi:10.1016/j.electacta.2012.03.070.

[22] J. Clavilier, R. Faure, G. Guinet, R. Durand, Preparation of monocrystalline Pt microelectrodes and electrochemical study of the plane surfaces cut in the direction of the {111} and {110} planes, J. Electroanal. Chem. Interfacial Electrochem. 107 (1979) 205–209. doi:10.1016/S0022-0728(79)80022-4.

[23] P.K. Glasoe, F.A. Long, Use of Glass Electrodes to Measure Acidities In Deuterium Oxide 1,2, J. Phys. Chem. 64 (1960) 188–190. doi:10.1021/j100830a521.

[24] A.K. Chandra, M.T. Nguyen, T. Zeegers-Huyskens, Theoretical Study of the Interaction between Thymine and Water. Protonation and Deprotonation Enthalpies and Comparison with Uracil, J. Phys. Chem. A . 102 (1998) 6010–6016.

[25] K.K. Irikura, R.D. Johnson, R.N. Kacker, Uncertainties in scaling factors for ab initio vibrational frequencies, J. Phys. Chem. A. 109 (2005) 8430–8437. doi:10.1021/jp052793n.

[26] A. Leœ, L. Adamowicz, M.J. Nowak, L. Lapinski, The infrared spectra of matrix isolated uracil and thymine: An assignment based on new theoretical calculations, Spectrochim. Acta Part A Mol. Spectrosc. 48 (1992) 1385–1395. doi:10.1016/0584-8539(92)80144-L.

[27] V. Zamlynny, J. Lipkowski, Quantitative SNIFTIRS and PM IRRAS of Organic Molecules at Electrode Surfaces, in: R.C. Alkire, D.M. Kolb, J. Lipkowski, P. Ross (Eds.), Adv. Electrochem. Sci. Eng., Wiley-VCH Verlag GmbH, 2006: pp. 315–376. doi:10.1002/9783527616817.ch9.

Table I

Table I: Experimental absorption frequencies of thymine spectra in D_2O solutions and in H_2O solutions and DFT calculated vibration frequencies for neutral and anionic deprotonated thymine in N_1 and in N_3 The main contributions of single vibrations to the calculated frequencies are included.(w-weak , m-medium, s-strong, str-stretching, bend- bending)

D_2O				
Exp. pD=1-7	Calc. $ThyD_2$	Exp. pD=12	Calc. $ThyD^-.(N_1)$	Calc. $ThyD^-.(N_3)$
2961 cm^{-1}	w-3122 cm^{-1} str C5H	2958 cm^{-1}	3004 cm^{-1} asym str - CH3	3050 cm^{-1} str C5H
2924 cm^{-1}	w-3057cm^{-1} asym str -CH3	2924 cm^{-1}	2971cm^{-1} str C5H	3001 cm^{-1} asym str - CH3
2852 cm^{-1}	w-2972cm^{-1} sym str -CH3	2857 cm^{-1}	2961cm^{-1} sym str - CH3	2932 cm^{-1} sym str - CH3
1695 cm^{-1}	s- 1741 cm^{-1} str C2O	1658 cm^{-1}	s-1635 cm^{-1} str C4O + C2O	m 1655 cm^{-1} str C5C6-C2O
1673 cm^{-1}	s- 1688 cm^{-1} str C4O	1606 cm^{-1}	s- 1597 str C4O - C2O	m 1624 cm^{-1} str C2O+C4O+C5C6
1652 cm^{-1} 1625 cm^{-1}	w- 1641 cm^{-1} str C5C6	1545 cm^{-1}	m-1550 cm^{-1} str C5C6	s-1543 cm^{-1} str C4O
H_2O				
Exp. pH=1-7	Calc. $ThyH_2$	Exp. pH=12	Calc. $ThyH^-.(N_1)$	Calc. $ThyH^-.(N_3)$
1704 cm^{-1}	s- 1754 cm^{-1} (1685) str C2O, bend N1H + N3H,	1600 cm^{-1} (wide)	s-1636 cm^{-1} Sym. str C4O + C2O	s-1657 cm^{-1} str C4O-C2O-C5C6
(sh)1690 cm^{-1}	s- 1699 (1302) str C4O, bend. N3H		vs- 1618 Asym. str C4O + C2O, bend N3H,	m 1637 cm^{-1} str C4O + C5C6
1666 cm^{-1}	w-1641 str C4C6		m 1552 cm^{-1} str C5C6	s 1548 cm^{-1} str C4O-C2O-C5C6
	w-1452 cm^{-1} ring breath., bend N1H			

Table II

Table II: Experimental ATR-SEIRA spectra frequencies of chemisorbed thymine from D_2O solutions and from H_2O solutions, and DFT calculated vibrations for anionic thymine tautomers N3 and N1 adsorbed on 19 gold atoms clusters, after optimization of the geometry.

D_2O				H_2O			
ATR-SEIRA spectra		Calculated vibrational frequencies		ATR-SEIRA spectra		Calculated vibrational frequencies	
pD=1	pD=12	N3 tautomer	N1 tautomer	pH=1	pH=12	N3 tautomer	N1 tautomer
3070 cm^{-1}	3070 cm^{-1}	w-3101 cm^{-1} str ‗CH	w-3051 cm^{-1} νas -CH3 (in plane)	3072 cm^{-1}		w-3101 cm^{-1} str CH	w-3051 cm^{-1} as. str CH3 (in plane)
2985 cm^{-1}	2977 cm^{-1}	w-3032 cm^{-1} asym- str CH3 -in plane	w-3039 cm^{-1} str C5H	2973 cm^{-1}		w-3032 cm^{-1} as str CH3 (in plane)	w-3038 cm^{-1} str C5H
2962 cm^{-1} (sh)	2926 cm^{-1}	w-2959 cm^{-1} sym. str -CH3	w-2954 cm^{-1} sym str CH3	2931 cm^{-1}		2959 cm^{-1} Sym str ‗CH3	2956 cm^{-1} Sym str CH3
1648 cm^{-1}	1631 cm^{-1}	s-1642 cm^{-1} str -C5C6+bend. CH	s-1624 cm^{-1} str C4O	1656 cm^{-1}	1643 cm^{-1}	s-1645 cm^{-1} str -C5C6, bend CH	s-1639 cm^{-1} str C4O, bend N3H
1581 cm^{-1} 1567 cm^{-1} (sh)	1574cm^{-1}	s-1586 cm^{-1} str ‗C2O +-C4O		1597 cm^{-1}	1558 cm^{-1}	s-1599 cm^{-1} str C2O+ C4O, bend N1H	w-1567 cm^{-1} str -C2O, bend N3H
	1527 cm^{-1}		w-1558 cm^{-1} str C2O+ bend CH		1506 cm^{-1}		vw-1493 cm^{-1} str -C5C6-C2C3 bend CH3
1478 cm^{-1}		w-1463 cm^{-1} bend CH3+CH	vw-1483 cm^{-1} str C5C6, bend CH3+CH	1490 cm^{-1}		m-1463 cm^{-1} bend CH3 + CH	
1440 cm^{-1}		s-1414 cm^{-1} str C4O+C2O	w-1445 cm^{-1} bend CH3 + CH			W – 1447 cm^{-1} bend N1H	w-1445 cm^{-1} bend CH , CH3
1407 cm^{-1}	1413 cm^{-1}	m-1393 cm^{-1} ring brth	w-1393cm^{-1} ring brth		1390 cm^{-1}	m-1410 cm^{-1} str ‗C4O	w-1399 cm^{-1} ring brth

Figure Legends

Scheme 1.- Acid-base equilibrium of thymine and tautomerism of its deprotonated form.

Scheme 2.- Optimized geometries of deprotonated N3 (2a) and N1 (2b) thymine on 19 gold atoms surface.

Scheme 3.- Transition dipole directions of the CH stretching (green dash-dot line), antisym. CH_3 stretching (red dotted line) and symmetric CH_3 stretching (blue dashed line) vibrational modes, and permanent dipoles vectors (grey arrow) for deprotonated thymine N3 (3a) and N1 (3b).

Figure 1.- Cyclic voltammetry of Au(111) electrodes in 1 mM thymine solutions at the indicated pH values. Scan rate = 50 mV s^{-1}.

Figure 2.- IR absorption spectra of 10mM thymine solutions in deuterated (2a) and non-deuterated (2b) aqueous media at pH 1 (blue solid line), pH 7 (red dashed line) and pH 12 (green dash dot line).

Figure 3.- ATR-SEIRA spectra, in the 1400 – 1700 cm^{-1} range, of thymine adsorbed on gold electrodes at potentials higher than the onset of the chemisorption from D_2O (Fig 3a) and from H_2O (Fig 3b) solutions at the indicated pH values. The absorption spectra of thymine solutions at the same conditions are shown for comparison. The ATR-SEIRAS at pD 7 in Fig 3a includes a linear combination (dashed line) of the spectra at pD 1 and pD 12.The potential values in Fig 3a are 0.7 V,0.5 V, and 0.2V for the experiments at pD 1, pD 7 and pD 12, respectively. In Fig. 3b the potential values are 0.7 V, 0.5 V, and 0.2 V for the experiments at pH 1, pH 7 and pH 12, respectively.

Figure 4.- ATR-SEIRA spectra, in the 2800-4000 cm^{-1} region, of thymine adsorbed on gold electrodes at potentials higher than the onset of the chemisorption from D_2O at the indicated pH values. The figure includes the results from the deconvolution of the experimental signals. The potential values are the same as in Fig 3a

Figure 5.- ATR-SEIRAS of thymine adsorbed on gold electrodes at indicated potential values from D_2O solutions at pD 1 (Fig 5a) and pD 12 (Fig 5b).

Figure 6.- ATR-SEIRA integrated intensities of the vibrational bands corresponding to CH stretching (green circles) and antisymmetric CH_3 stretching (red inverted triangles) vibrations related to symmetric CH_3 stretching of thymine adsorbed at pD 1 (Fig 6a) and at pD 12 (Fig 6b).

Scheme_1

Click here to download high resolution image

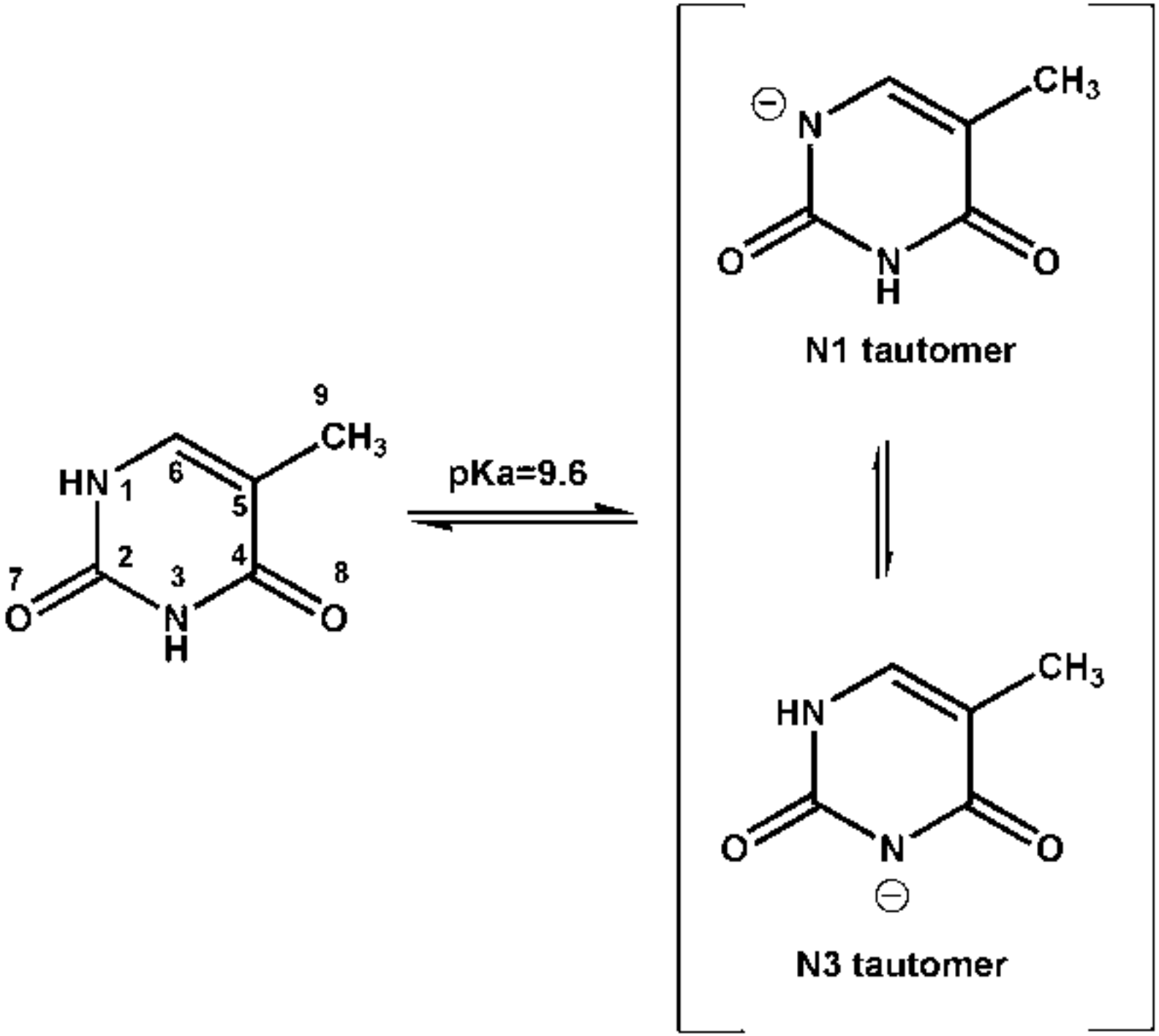

Scheme_2a

Click here to download high resolution image

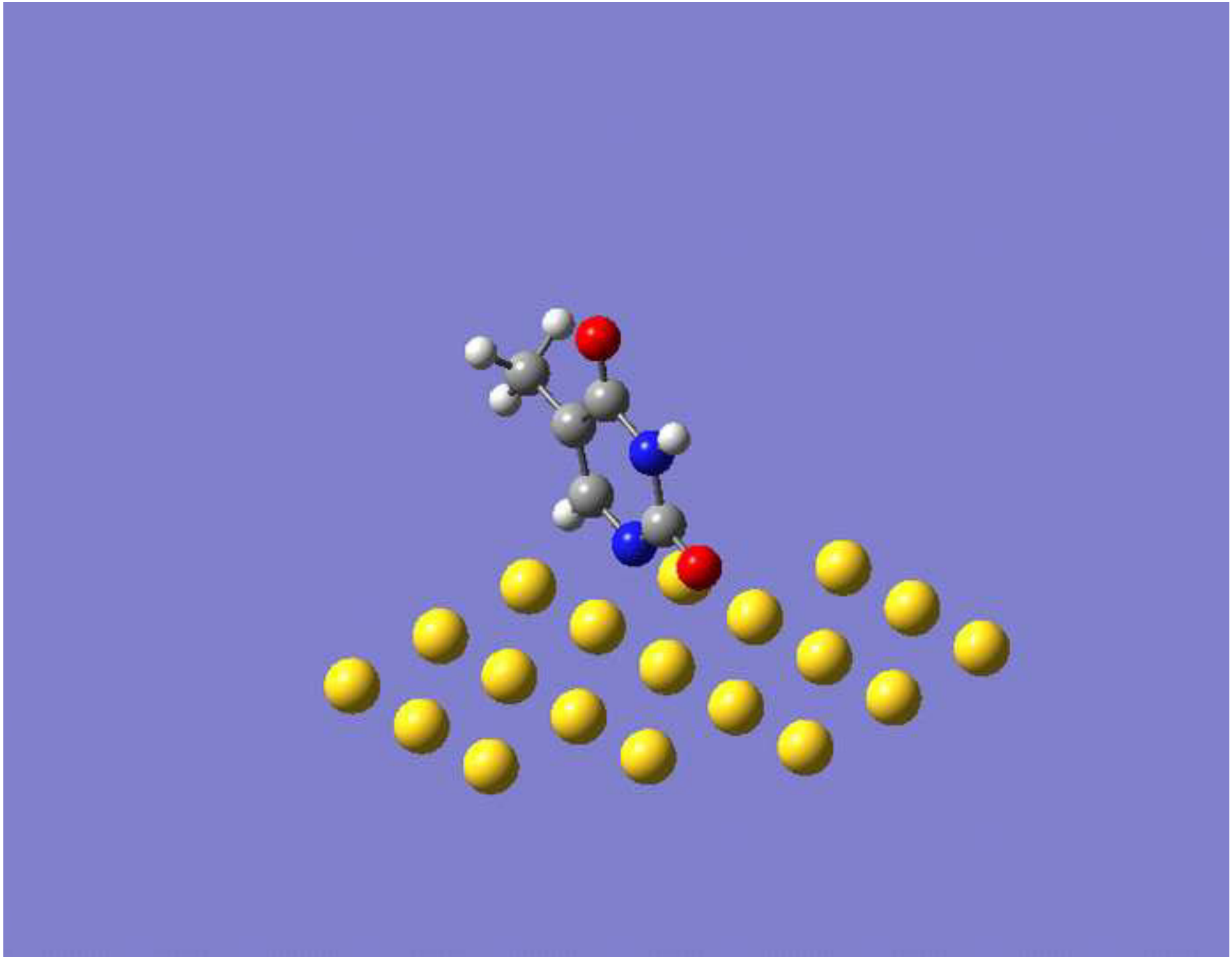

Scheme_2b

Click here to download high resolution image

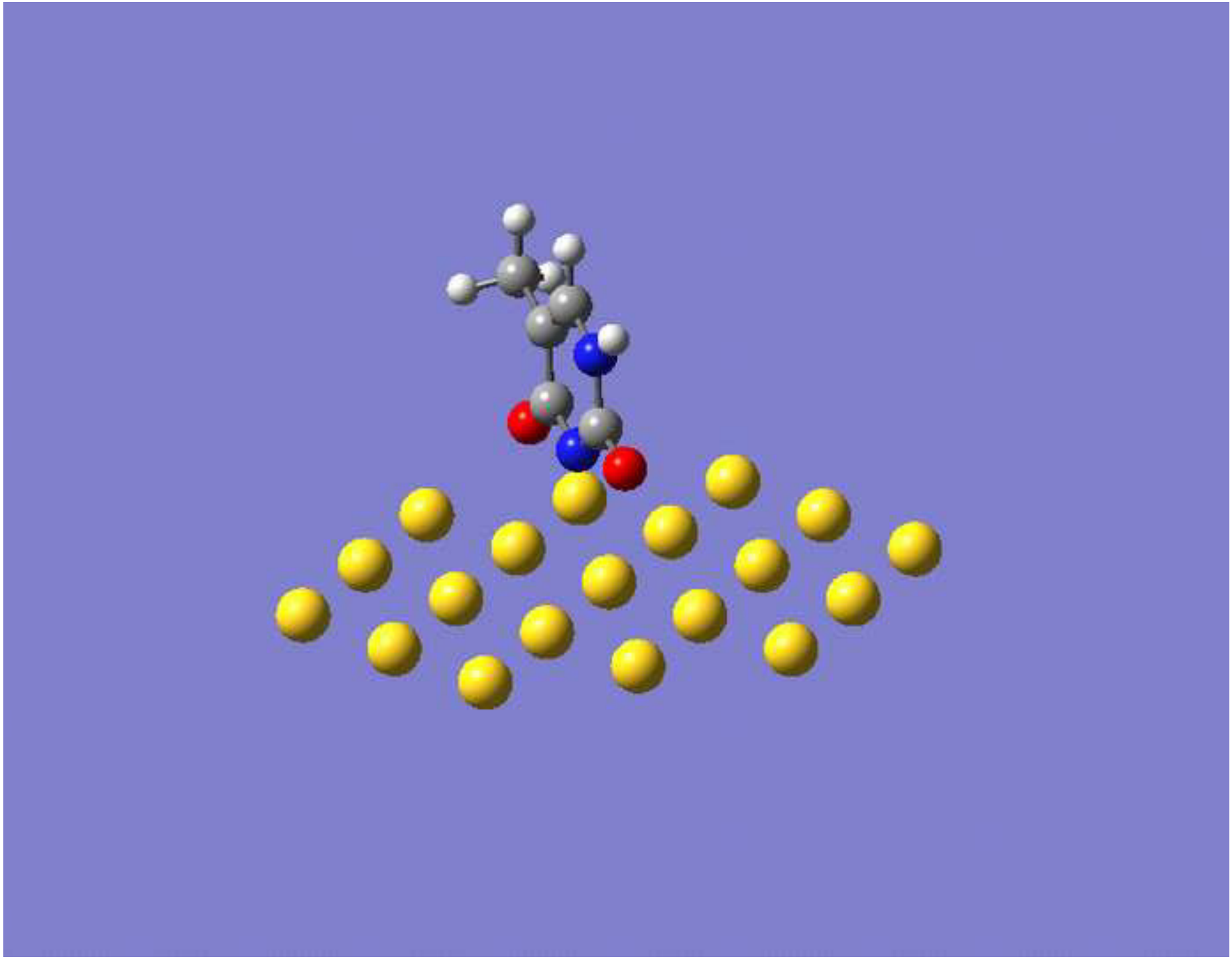

Scheme_3a

Click here to download high resolution image

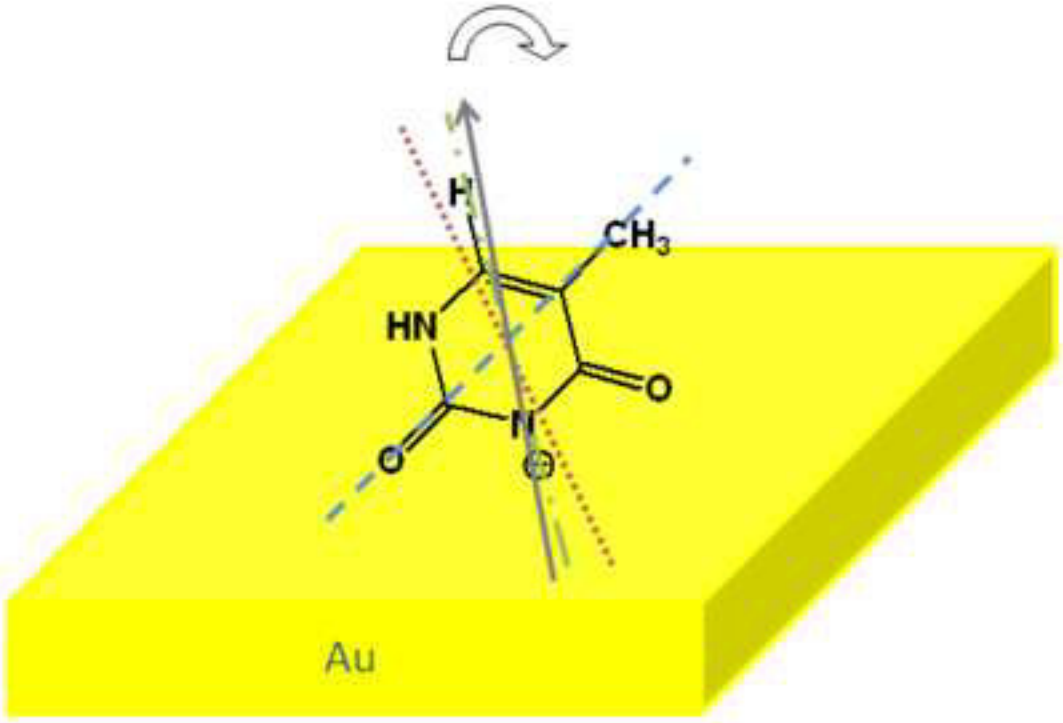

Scheme_3b

Click here to download high resolution image

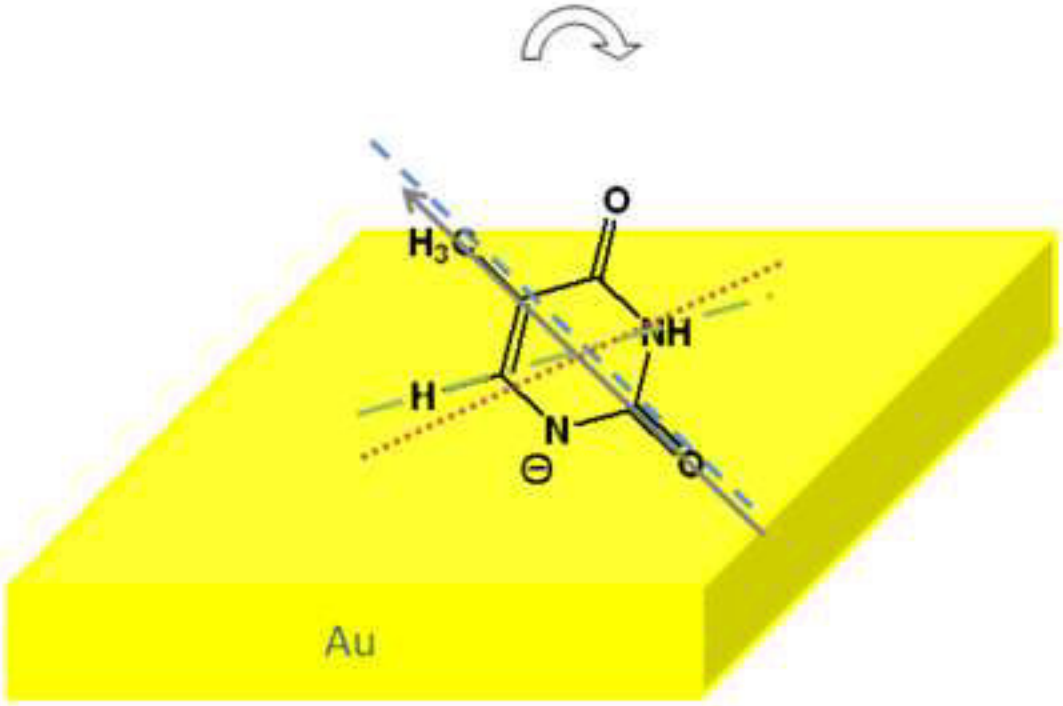

Figure 1
Click here to download high resolution image

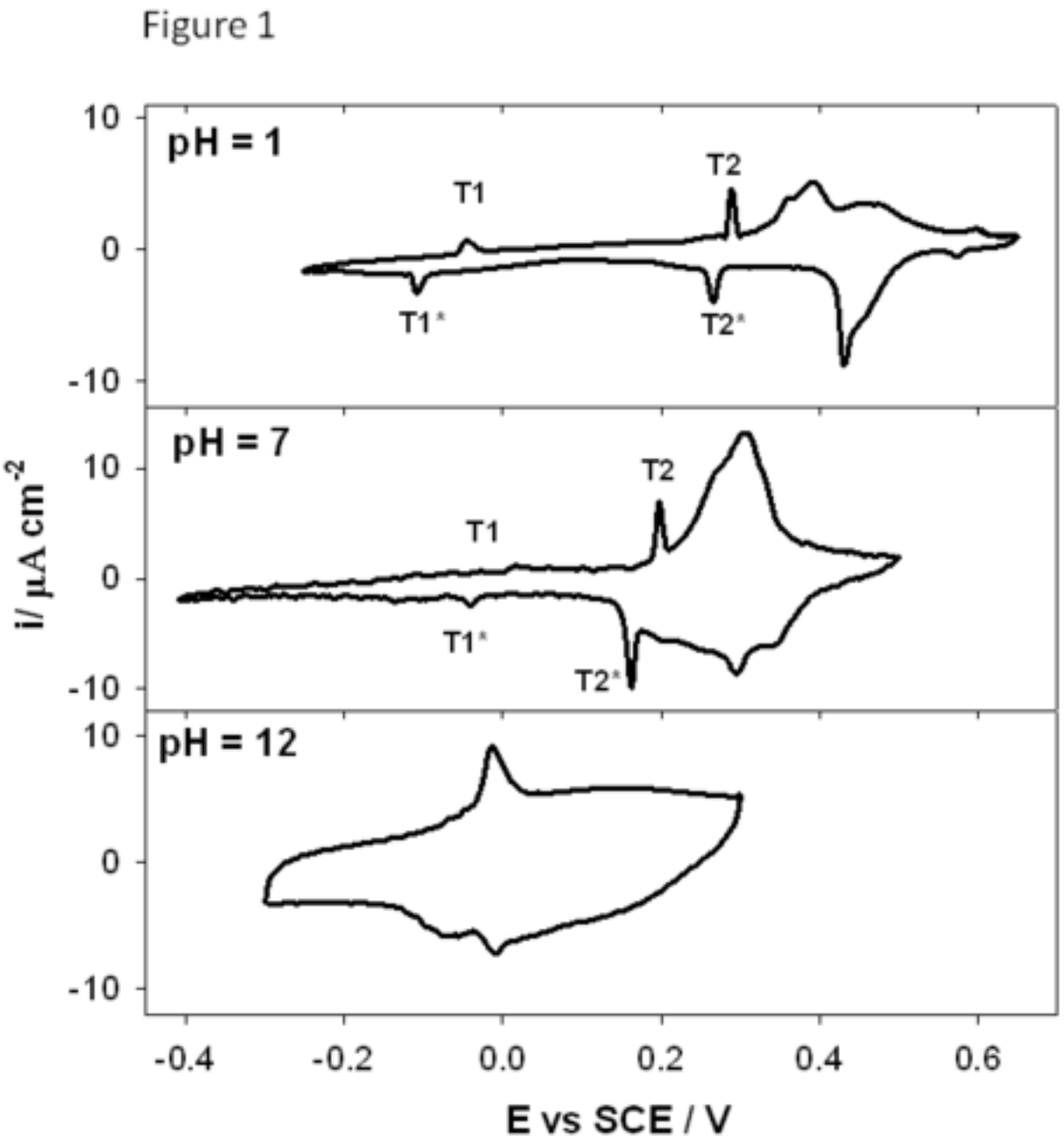

Figure 2
Click here to download high resolution image

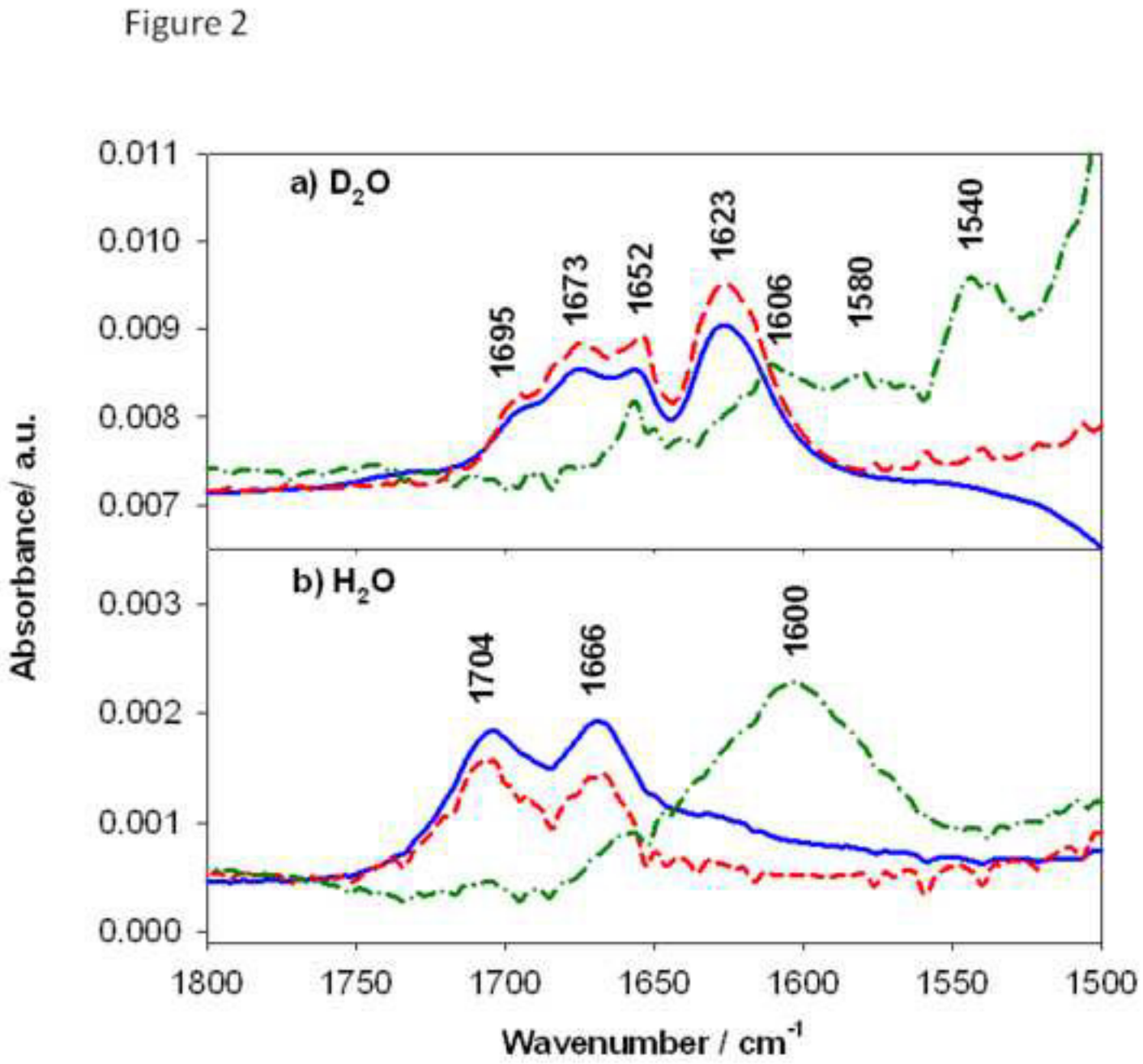

Figure 3a

Click here to download high resolution image

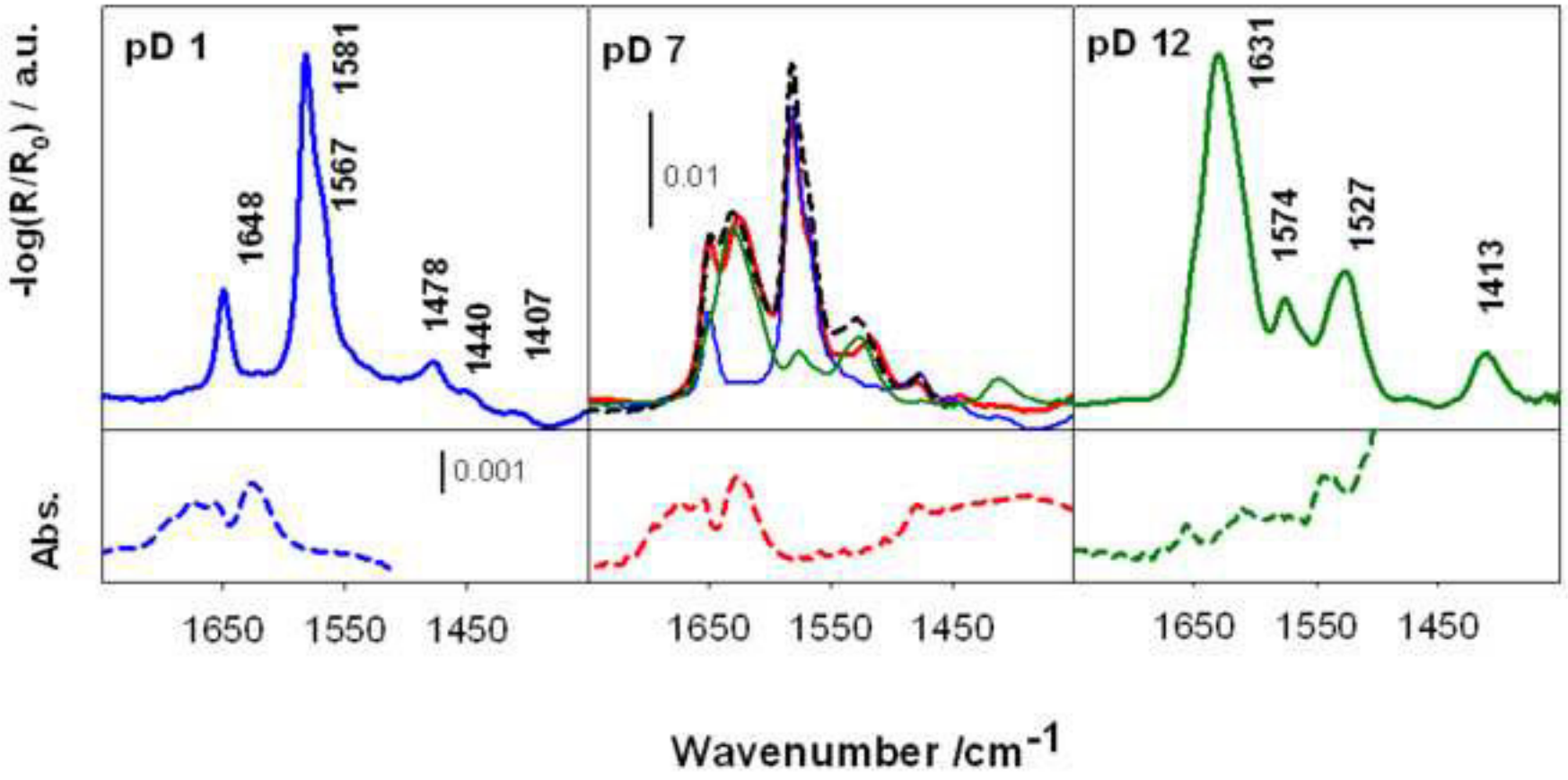

Figure 3b

Click here to download high resolution image

Figure 3b

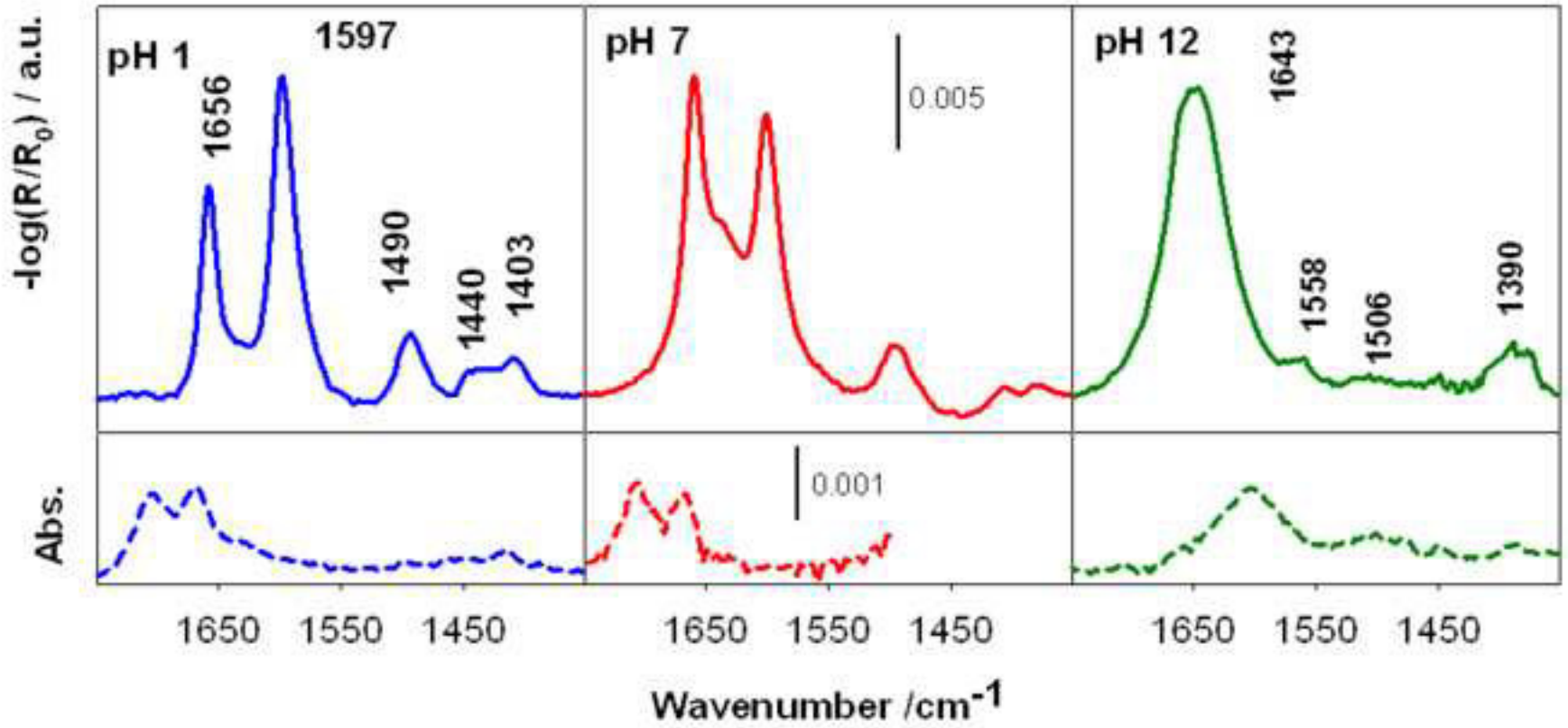

Figure 4
Click here to download high resolution image

Figure 4

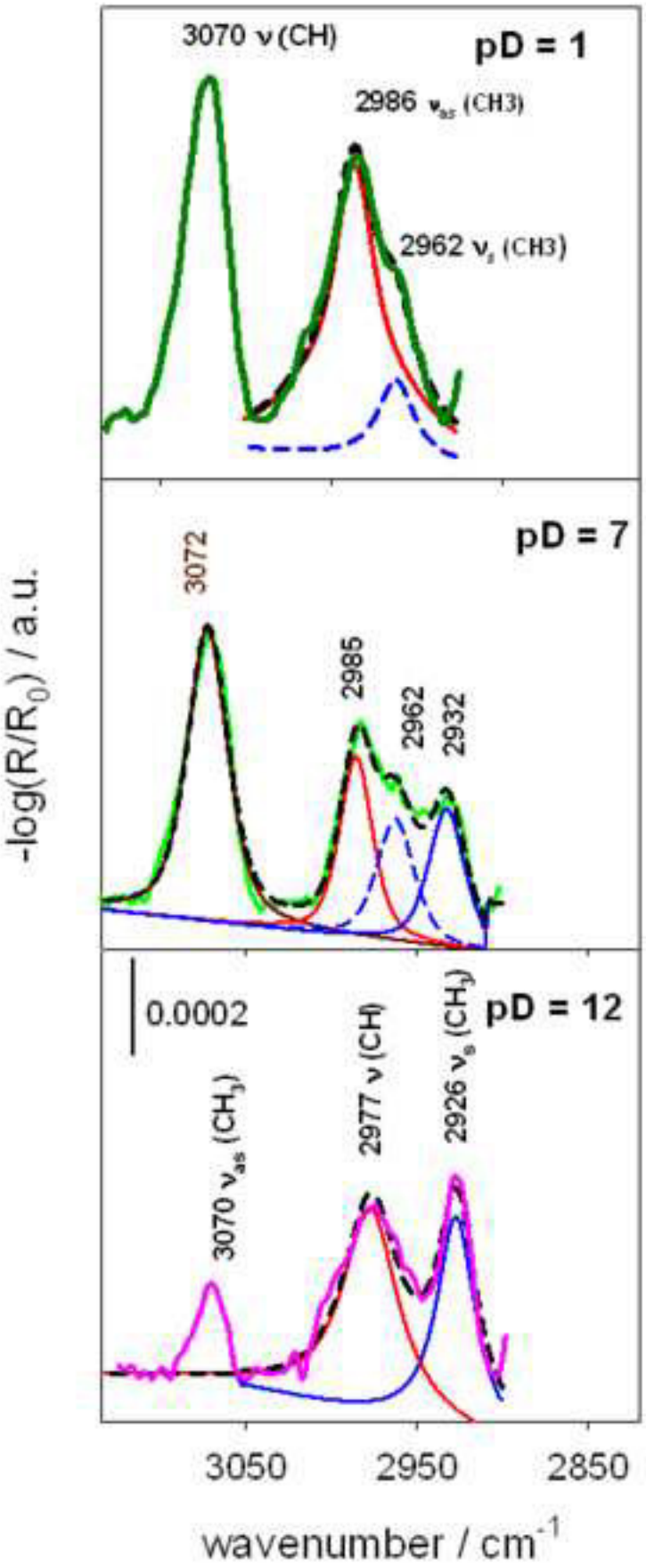

Figure 5a
Click here to download high resolution image

Figure 5a

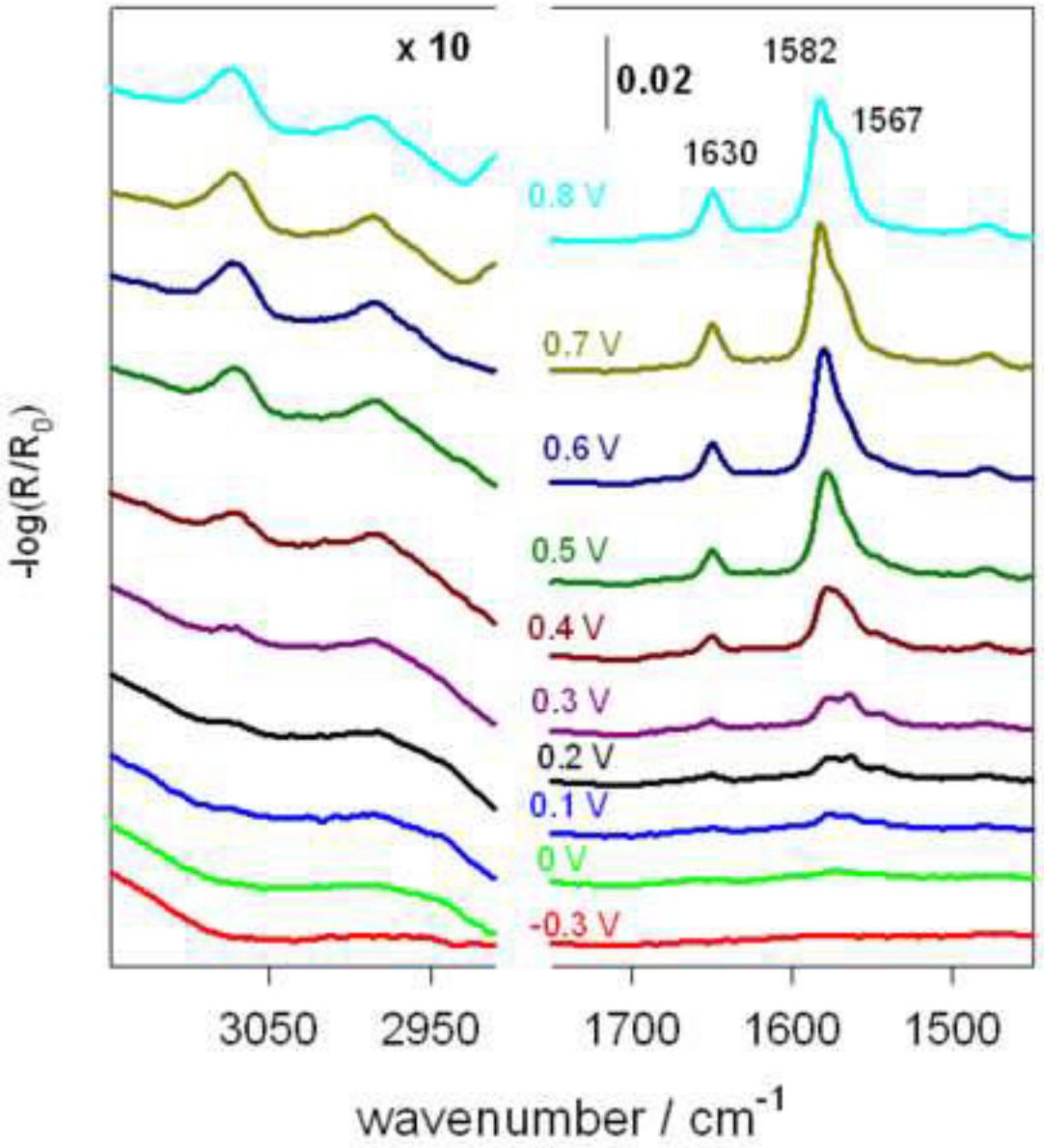

Figure 5b
Click here to download high resolution image

Figure 5b

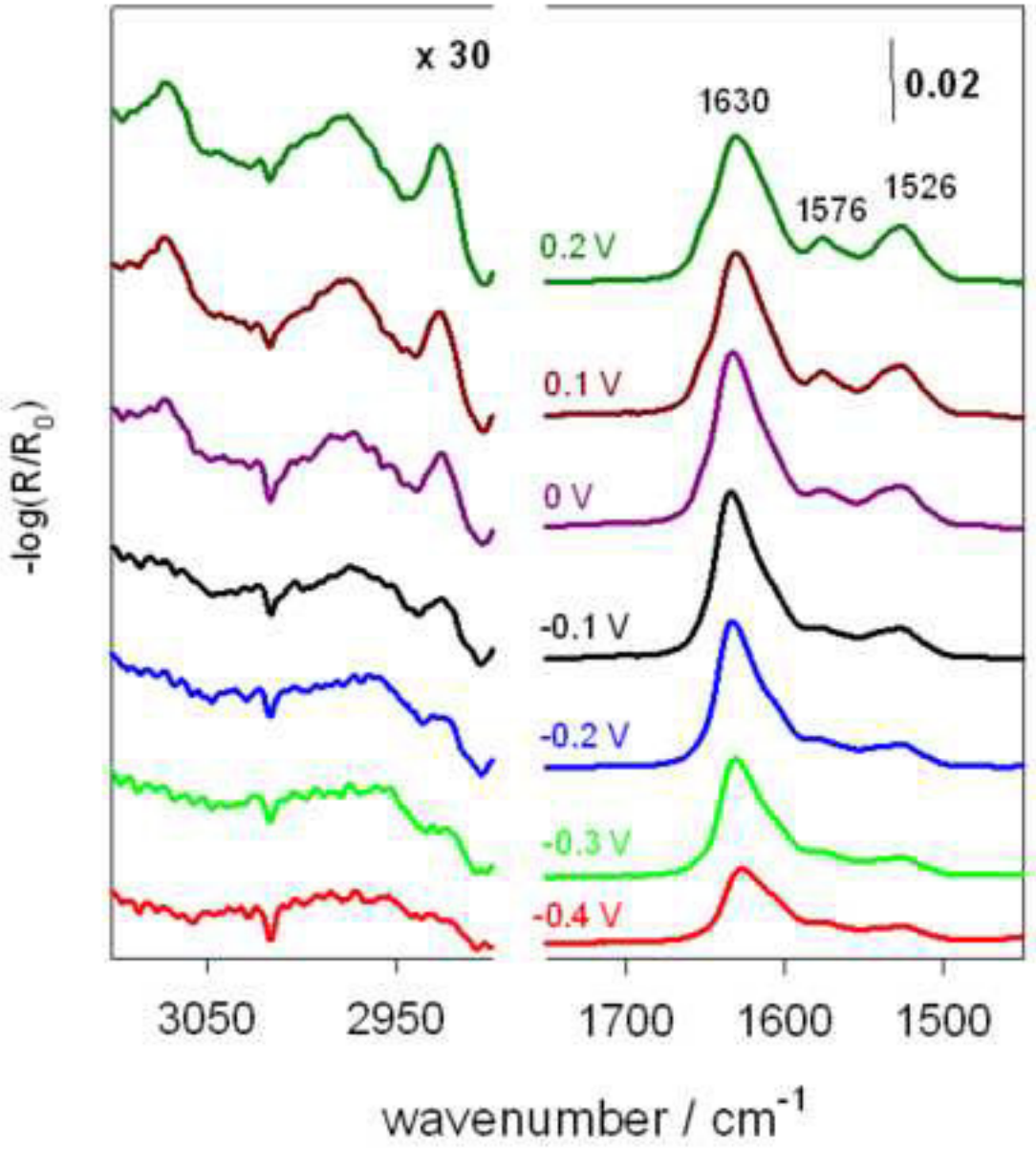

Figure 6a
Click here to download high resolution image

Figure 6a

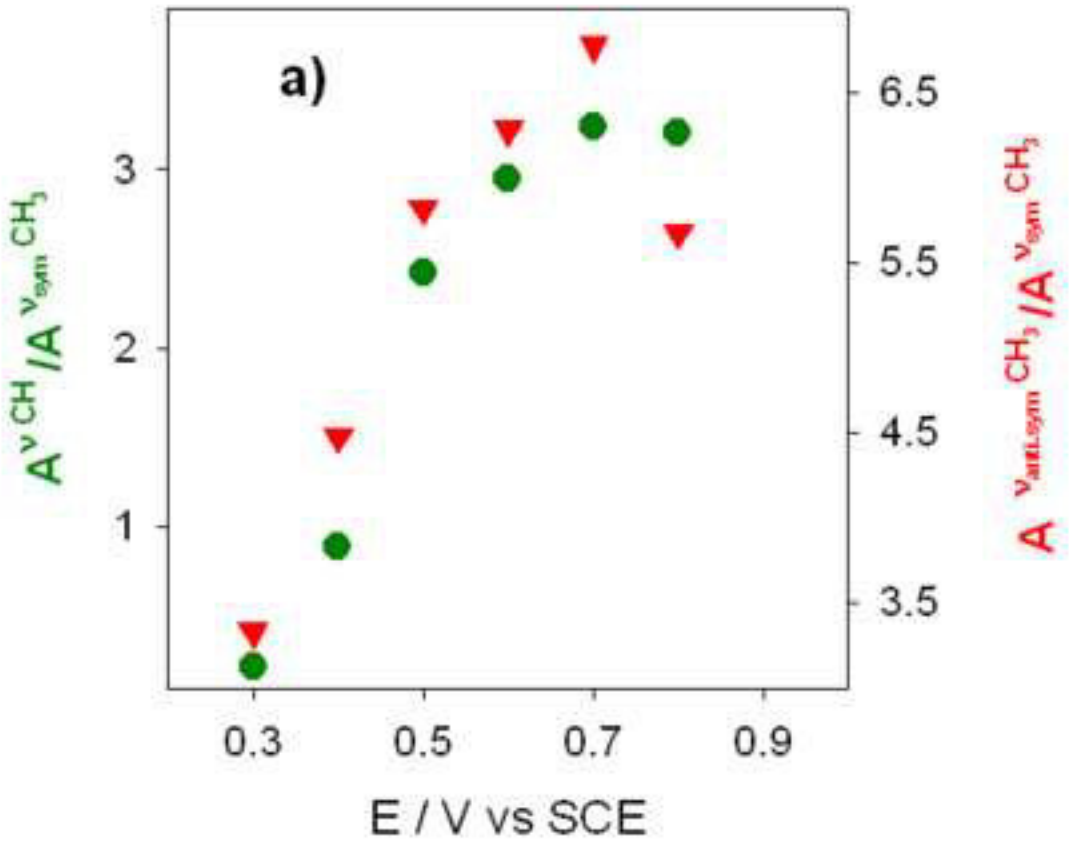

Figure 6b

Click here to download high resolution image

Figure 6b